

## Internal Tide in the Kara Gates Strait

E. G. Morozov<sup>a,\*</sup>, I. E. Kozlov<sup>b,c</sup>, S. A. Shchuka<sup>a</sup>, and D. I. Frey<sup>a</sup>

<sup>a</sup>*Shirshov Institute of Oceanology, Russian Academy of Sciences, Moscow, Russia*

<sup>b</sup>*Russian State Hydrological University, St. Petersburg, Russia*

<sup>c</sup>*Klaipėda University, Klaipėda, Lithuania*

\**e-mail: egmorozov@mail.ru*

Received February 19, 2016

**Abstract**—We observed strong internal tidal waves in the Kara Gates Strait. Internal tides are superimposed over a system of mean currents from the Barents to the Kara Sea. Field studies of internal tides in the Kara Gates were performed in 1997, 2007, and 2015. In 2015, we analyzed data from towed CTD measurements, numerical model calculations, and satellite images in the region. An internal tidal wave with a period of 12.4 h is generated due to the interaction between the currents of the barotropic tide and the bottom relief on the slopes of a ridge that crosses the strait from Novaya Zemlya to the continent. The depths of the ridge crest are 30–40 m. A constant current of relatively warm water flows from the Barents to the Kara Sea. An internal wave propagates in both directions from the ridge. In the Barents Sea, internal waves are intensified by the current from the Barents to the Kara Sea. Internal bores followed by a packet of short-period internal waves are found in both directions from the strait. Satellite images show that short-period internal waves are generated after the internal bore. A hydraulic jump was found on the eastern side of the strait. Numerical modeling agrees with the experimental results.

DOI: 10.1134/S0001437017010106

### INTRODUCTION

For almost 20 years, the Shirshov Institute of Oceanology, Russian Academy of Sciences, has systematically studied internal waves in the Kara Gates Strait. These studies began in 1997, when three buoys were moored in the strait [7, 15]; a hydrological survey was conducted. The studies were continued in 2007. A transect with a towed CTD sounder in the scanning mode was made through the strait [14]. In 2015, along and across the strait, CTD sounding measurements in the scanning mode were continued. Figure 1 shows the scheme of the studies in different years.

The Kara Gates Strait is overlain by an underwater ridge, the crest of which reaches depths of 35–40 m. On both sides of the ridge is a steep drop-off to depths of 200 m or more. These relief data were obtained during several crossings of the strait and the placement of moorings in it. The measured data sharply differ from the body of digital data [19]. According a depth map constructed from Internet data [43] ([http://topex.ucsd.edu/cgi-bin/get\\_data.cgi](http://topex.ucsd.edu/cgi-bin/get_data.cgi); <http://www.ngdc.noaa.gov/mgg/global/global.html>), the depths around the strait are close to 50 m and do not exceed 100 m. This body of bathymetry data does not correspond to reality and can introduce errors in model calculations.

It is well known [10] that the average current in the Kara Gates is directed from the Barents to the Kara Sea. From buoy observations in 1997, the current velocity

at the core is within the limits of 6–26 cm/s and the maximum velocity reaches 50 cm/s. In 1997, in the strait according to buoy measurement data, a backflow of bottom water was detected similar to the lower current in the Strait of Gibraltar. The measured average current velocities were 11 cm/s (maximum velocity, up to 43 cm/s) at a depth of 215 m over an ocean depth of 230 m in the southeastern part of the strait. There is a weak surface current from the Kara Sea around the southeastern end of Novaya Zemlya, which generates the Litke Current along the western coast of the archipelago [13]. Both backflows are significantly weaker than the flow into the Kara Sea.

The authors of [10] write that the flow of warm water from the Barents into the Kara Sea intensifies in winter. The maximum transport reaches 0.65 Sv. In summer, north winds predominate and decrease this flow. According to their data, the mean flow per year is 0.3 Sv. The authors of [18] analyzed internal wave measurements in the Kara Sea and demonstrated that internal waves were observed only in summer, when there was stratification.

The flow velocity amplitude of the barotropic tide, according to calculations based on satellite altimetry data, is 9 cm/s [15]. The modeling in [15] yields good coincidence with the current and tidal dynamics in the Kara Gates.

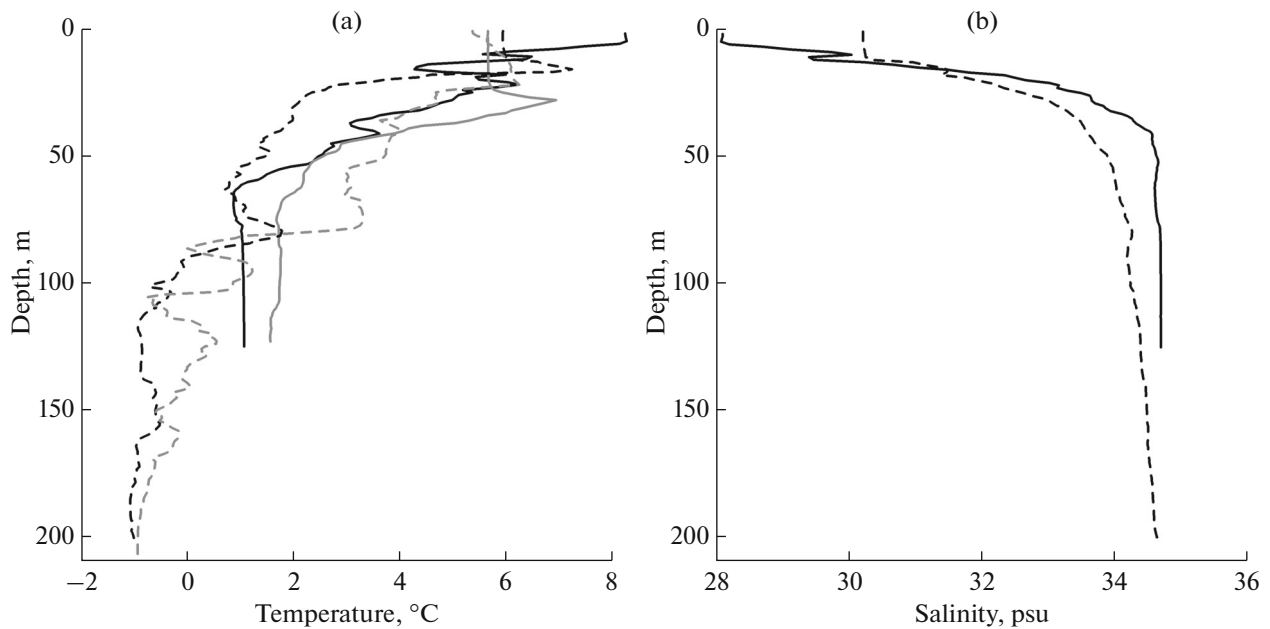


**Fig. 1.** (a) Temperature and (b) salinity profiles in area of Kara Gates Strait. Station 5196-1 (Barents Sea), black solid line; station 5197-1 (Kara Sea), gray solid line; station 5196-2 (Barents Sea), black dotted line; station 5197-2 (Kara Sea), gray dotted line.

According to the data of earlier studies [7, 14, 15], it is possible to describe the internal tidal waves in the Kara Gates Strait as follows. The internal tide amplitudes in the area of the strait are extremely large and, according to mooring data, in spring tides, water particles can execute vertical motions with a spread of up to 70 m. The mechanism by which the internal tide is generated in the strait is similar to that in other straits. A close similarity to the wave dynamics of the strait has been detected in the straits of Gibraltar and Bab-el-Mandeb [6, 15, 16]. The interaction with currents intensifies fluctuations.

In 2007, measurements were conducted in the strait with an Idronaut 316 CTD profiler in the scanning mode [14]. In that study, it was shown that the measurement results agreed with numerical model calculations of internal waves. In addition, during propagation of an internal tide to the west in the Barents Sea counter to the main current flow, the internal tide is intensified and intense waves break, generating high-frequency internal waves. Surface manifestations of these waves were recorded by radar observations.

In 2015, towed CTD measurements were repeated and expanded. The aim of this work is to analyze the new results together with satellite observations of surface manifestations of internal waves and numerical modeling.

#### HYDROLOGICAL BACKGROUND DURING OPERATIONS

To determine the hydrological background during the 2015 studies on cruise 63 of the R/V *Akademik Mstislav Keldysh*, four SBE-19 CTD stations were occupied on both sides of the strait. Data on the stations are given in the table. Figure 1 shows the temperature and salinity plots. The water temperature on the Kara side on the whole was lower than on the Barents side, especially in the deep-water part. For the 38 days that elapsed between measurements, cooling of the upper layer up to 20–30 m was observed, especially from the Barents side. In the upper layer of the Barents Sea, desalination of water was noticeable, apparently due to runoff from the Pechora River and

#### CTD stations in strait

Station no.; date	Latitude, N	Longitude, E	Depth, m
5196-1; 28.08.2015	70°12.2′	057°34.0′	128
5197-1; 29.08.2015	70°53.3′	059°01.0′	209
5197-2; 06.10.2015	70°53.2′	059°00.9′	205
5196-2; 07.10.2015	70°12.3′	057°34.2′	125

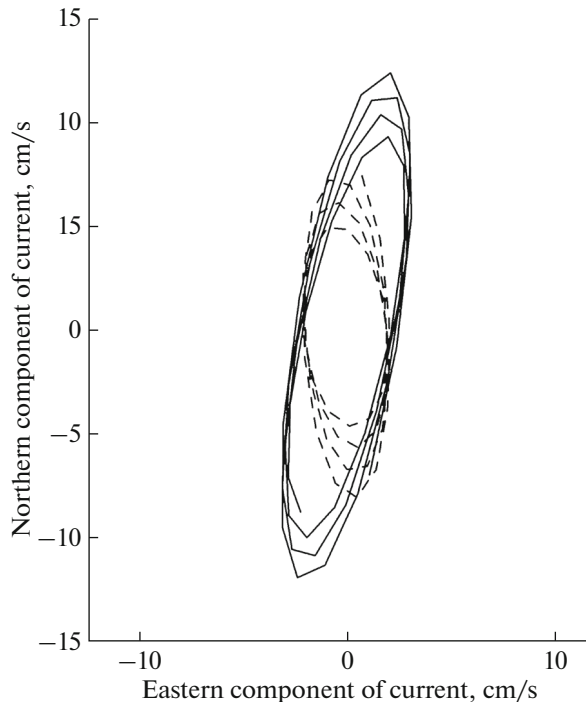


**Fig. 2.** Tidal ellipses M2 and S2 on August 28–29 (thick line) and October 6–7, 2015 (dotted line). Calculation from satellite altimetry with a sampling rate of 1 h.

transfer of desalinated waters by the current of the upper layer. In the Barents Sea in deep-water layers, fresher water than in the Barents Sea was detected. This can be explained by the large transfer of fresh waters from the Ob and Yenisei rivers, by wind mixing in summer, and convective mixing when the sea freezes in winter.

In studying tides and internal tidal waves, it is important to know the lunar phases. A full moon was observed on August 29 and September 28, a last quarter on October 5, and a new moon on September 13. There was a lunar eclipse on September 28 and a solar eclipse on September 13 in the polar regions of the Southern Hemisphere. Thus, the first stage of operations occurred during the spring tide, and the second stage began almost at the neap tide. The ellipses of tides M2 and S2 on the dates of the transects through the strait were calculated by assimilating satellite altimetry data with Oregon State University's OTPS algorithm of (<http://volkov.oce.orst.edu/tides/otps.html>) [9]. The ellipses are shown in Fig. 2. There is a noticeable increase in the velocities during spring tides and elongation of the ellipses along the strait. Velocities of the tide in the strait exceeding 10 cm/s are significantly larger than the usual 1–2 cm/s; therefore, strong internal tides are generated.

#### TOWED CTD SOUNDER MEASUREMENTS

Measurements were performed in the strait with a CTD profiler in the scanning mode. The first stage of

operations took place on August 28–29, and the second stage, on October 6–7, 2015. The towed device was based on an Idronaut 320 plus sounder in a well-streamlined and dynamically stabilized structure. The measurement rate was 27 cycles per second. The scanning mode was ensured by continuously varying the depth of the device. As the device moved, it was periodically lowered and raised with a winch at a rate of around 1 m/s from a depth of 1–2 m below the surface to a depth of 1 m from the bottom. Each cycle lasted around 5 min depending on depth. The horizontal resolution of measurements (departures of the device toward the surface) was several hundred meters depending on sea depth. The data on sea depth were derived from a Knudsen Chirp 3212 parametric echosounder.

During the studies, several measurement legs were completed in different directions along the strait from the Barents to the Kara Sea and back, as well as a leg across the strait. Measurements on August 28–29 were conducted from the point 70°12' N, 57°34' E to 70°45' N, 58°39' E. The diagonal leg was from the point 70°21' N, 58°23' E to 70°24' N, 57°41' E. The leg from the Kara to the Barents was made on October 6 from the point 70°45' N, 58°39' E to 70°12' N, 57°34' E. Figure 3 shows a diagram of the legs.

#### MEASUREMENT ANALYSIS

We estimated the length of a semidiurnal wave by integrating the equation for internal waves. In calculations, we assumed that the ocean bottom was flat far from the area of wave generation at the ridge in the strait and that, far from the slope, generation forces were absent. The wavelength can be estimated by numerically integrating the equation for the vertical velocity ( $w$ ) in an internal wave:

$$\frac{d^2 w}{dz^2} + \frac{N^2(z) dw}{g dz} + \frac{N^2(z) - \omega^2}{\omega^2 - f^2} w k^2 = 0, \quad (1)$$

where  $N(z)$  is the Brunt–Väisälä frequency calculated from the CTD data to the west and east of the strait,  $\omega$  is the semidiurnal frequency,  $f$  is the Coriolis parameter, and  $k$  is the horizontal wavenumber. For this problem (for the eigenvalues with a depth-variable buoyancy frequency), the boundary conditions for the vertical velocity are the zeros of the vertical velocity at the surface and at the bottom. The equation was integrated with a step of 10 m along the vertical. As a result of integration, we obtained the wavenumbers for different modes and the corresponding phase velocities of internal wave modes. The first mode has no zeros for depth (only zero velocities at the surface and bottom). The conditions of the model require an even bottom. In calculations, we assumed that the mean depth far from the strait from the Barents side was 120 m, and from the Kara side, 160 m. These depths are close to the average ones on the transects (Figs. 4, 5). The

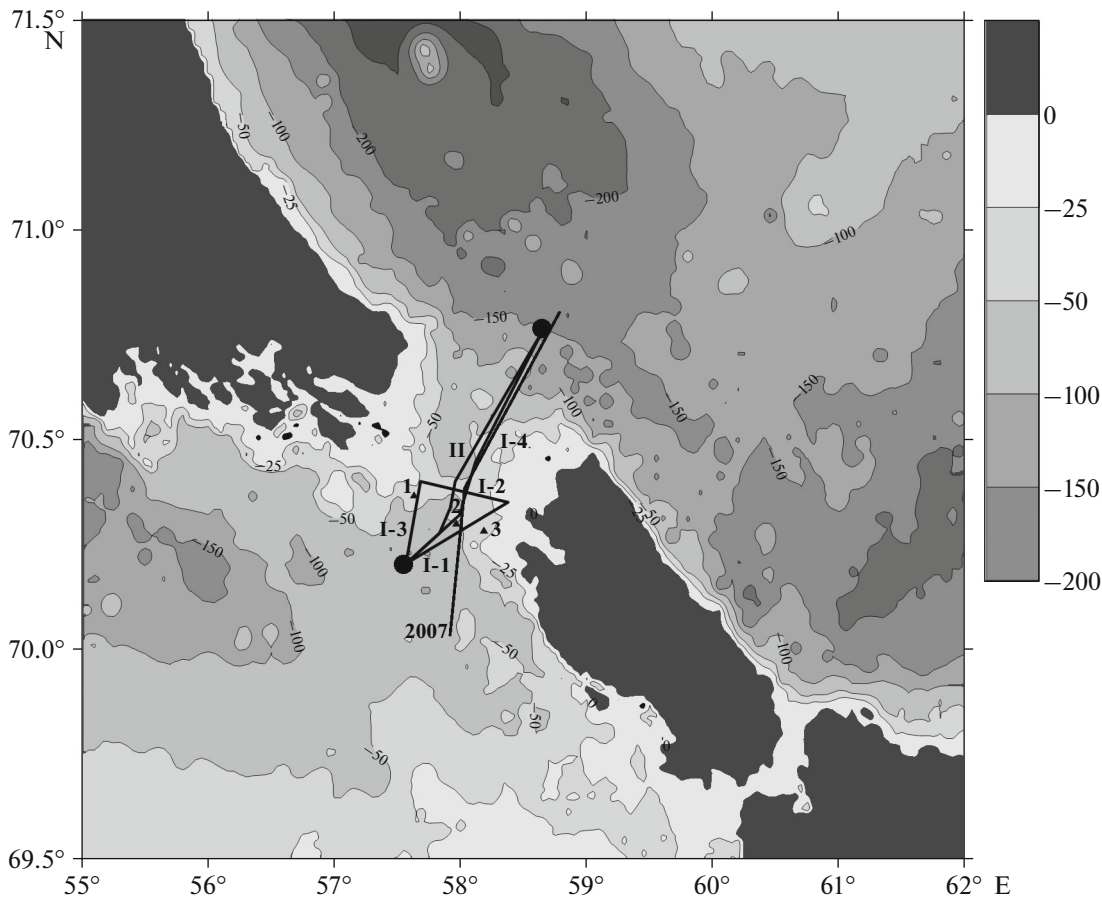


**Fig. 3.** Bathymetric map of study area in Kara Gates Strait from data set [19] (<http://www.ngdc.noaa.gov/mgg/global/global.html>), which differs sharply from real bathymetry directly near the strait. Shown are legs of scanning-sounder transects toward Kara Sea: I-1, I-2 (transverse); I-3, I-4 (along strait); return leg (II); 2007 leg; CTD sounding points (black dots) and buoy placement points in 1997 (triangles 1, 2, 3).

calculated value for the length of the half-line internal wave was 23000 m. Calculations were done for a zero mean current velocity.

From our scanning-mode sounding results, we constructed the temperature, salinity, and density profiles along and across the strait (Figs. 4–6). On profiles along the strait, we observed fluctuations in temperature and salinity caused by an internal tidal wave propagating into the Barents Sea (the Barents Sea in Figs. 4 and 5 is on the left). On the Kara side, we detected a hydraulic jump: deepening of the isothermic and isopycnic surfaces up to 100 m. In the western part of the transect, which was located in the Barents Sea, we observed characteristic fluctuations of the isothermic surfaces, which corresponded to the wavelengths. The internal tide was best differentiable by fluctuations of the 1.0–2.5°C isotherms. In terms of distances between the maximum deepening of the isotherms on the profiles closest to the ridge, a wave has a wavelength around 12 km; the next one, 15 km; and the third, 18 km. In the eastern part of the transect, we observed deepening of the isotherms to 100 m (the 1.5°C isotherm), which is a hydraulic jump as a

result of the mean current from the Barents Sea flowing around the ridge.

The transect was carried out from southwest to northeast (Fig. 3). On the Barents side, the vessel moved toward the propagating wave, which should have led to a reduction in the wavelength. The speed of the vessel  $U$  was 6 knots, i.e., 3 m/s. For a wavelength  $L = 23000$  m, the phase velocity  $c$  of the wave is close to 0.5 m/s. According to the Doppler effect, when the vessel moves toward the wave, the apparent wavelength decreases and increases if the wave is incidental as the vessel moves. Therefore, the wavelengths in the Barents and Kara seas will differ as the vessel moves in one direction.

The measured apparent period of the semidiurnal wave  $T_D$  will be

$$T_D = L/(c + U),$$

and the wavelength altered by the Doppler effect turns out to be

$$L_D = UT_D = \frac{LU}{c \pm U} = \frac{23000 \text{ m} \times 3 \text{ m/s}}{3.4 \text{ m/s}} = 20294 \text{ m},$$

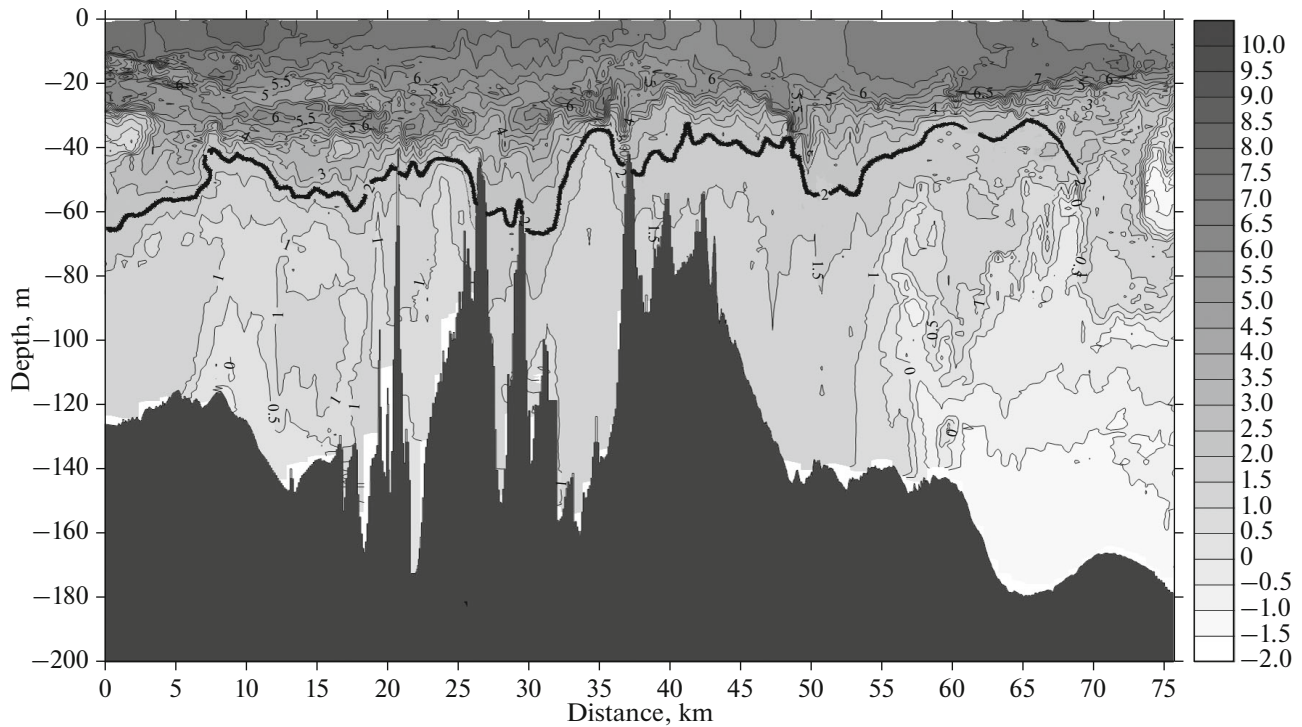


**Fig. 4.** Temperature distribution on towed CTD transect along strait during movement from Barents into Kara Sea. Isotherms drawn with 0.5°C interval. Bottom profile shown in dark gray. 2°C isotherm highlighted by thick line.

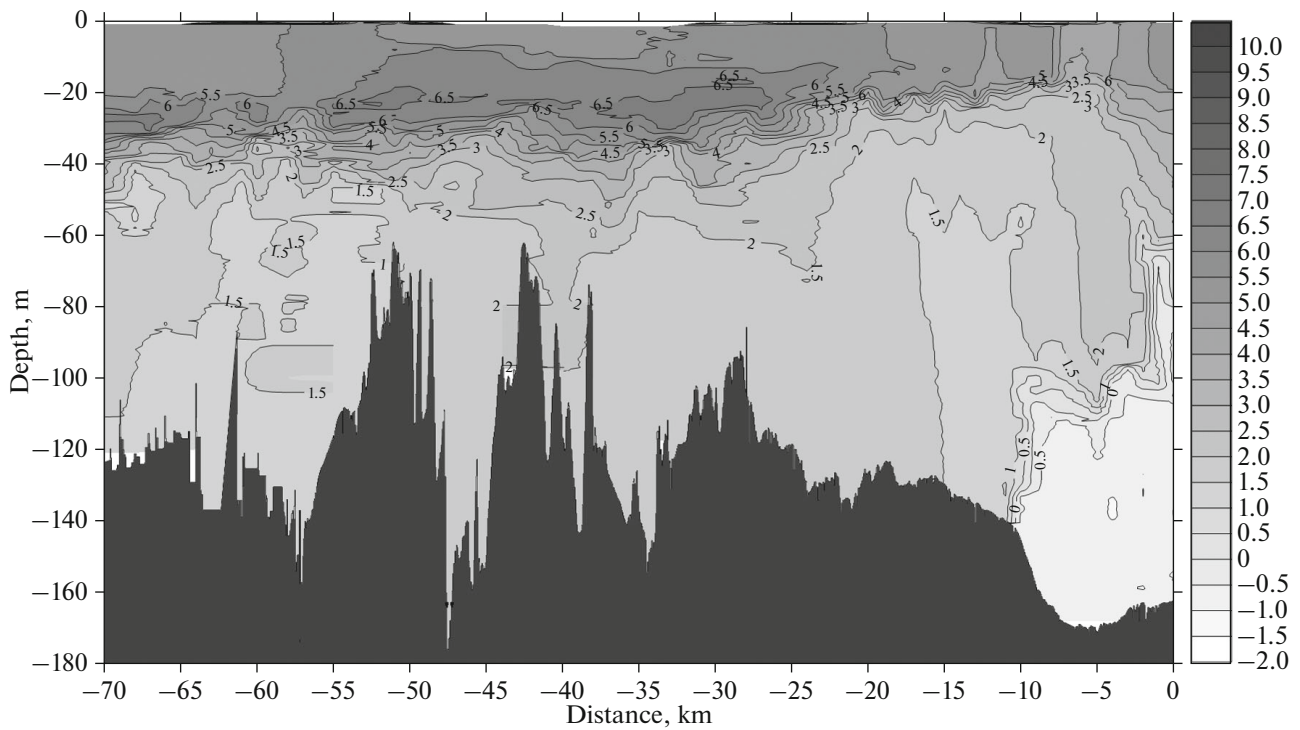


**Fig. 5.** Temperature distribution on towed CTD transect along strait for motion from Kara into Barents Sea. Isotherms drawn with 0.5°C interval. Bottom profile shown in gray.

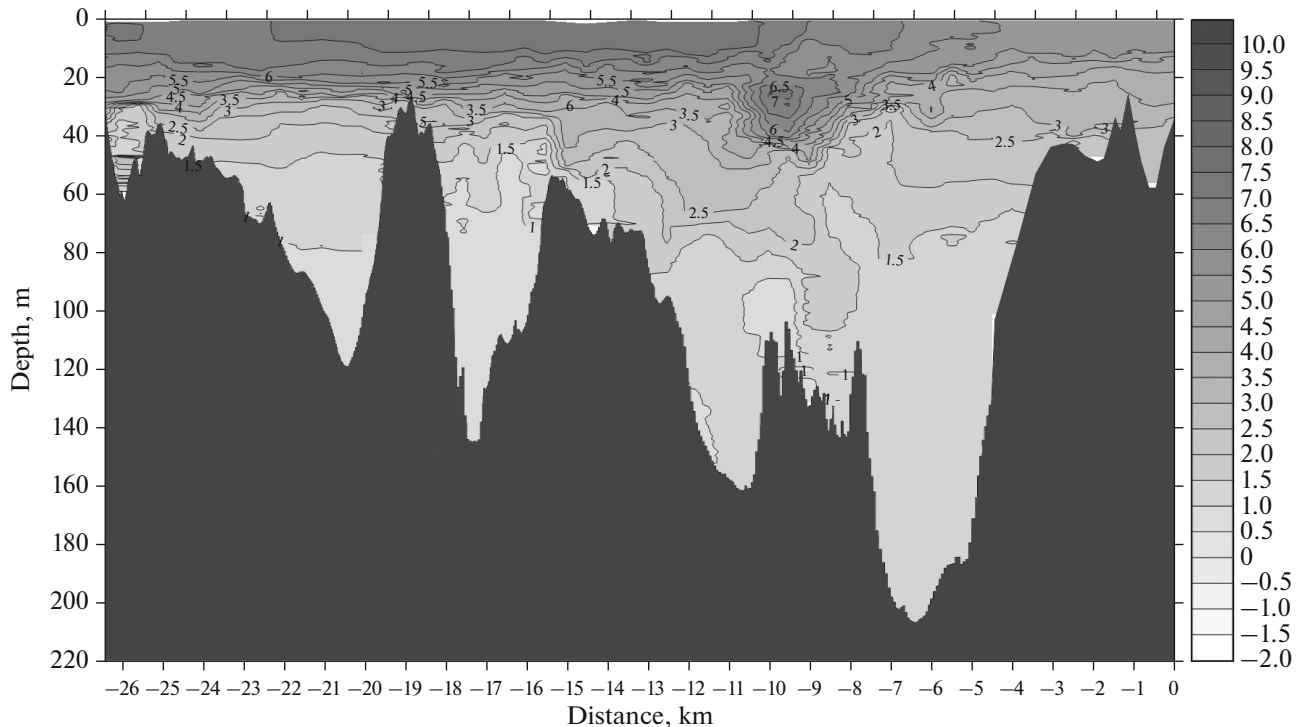


**Fig. 6.** Temperature distribution on towed sounder transect across strait. Isotherms drawn with 0.5°C interval. Bottom profile shown in gray.

which is close to the observed value. In the denominator, a plus sign is used, since the wave propagates toward the vessel's motion. A constant velocity in the entire ocean column opposite to wave propagation decreases the wavelength by 2 km.

The completion of legs along and across the strait showed unexpected sea depth values, which are not in the digital data files. Already during mooring deployment in 1997 and legs along the strait in 2007, it became clear that the digital depth data files [19] do not correspond to reality. During the execution of the transverse leg (I-2) in 2015 in the southeastern part of the strait, the presence of a channel with depths of more than 200 m was confirmed (Fig. 6). A buoy was deployed in this channel in 1997. During the transverse leg through the strait in 2015, three more channels were detected with smaller, but significant depths of 160, 150, and 120 m. In the southeastern channel, water temperatures in the deep-water part were higher than in the other channels, and the salinity was also higher. This reflects the fact that the main current from the Barents Sea goes through this southeastern channel. This is confirmed by the satellite image in Fig. 7. These underwater channels make it possible for currents in the strait to pass through the underwater ridge across the strait, which is a continuation of the Ural Mountains.

From the Kara Sea side, according to CTD measurements, an internal wave is visible with a length

around 25–27 km, but with a smaller amplitude than on the Barents side. According to towed CTD measurement data, a hydraulic jump is visible on the Kara side. The 1.5°C isotherm deepens from 50–60 m to 120 m. This frequently detected deepening of the isotherms manifests itself to a particular degree on the Kara side of the strait depending on the mean flow velocity.

The reverse leg took place on October 6–7. This was the neap tide period, and all the features of internal waves were less pronounced. The temperature profile from the towed sounder is shown in Fig. 5. On the Kara side, temperature fluctuations were detected, related to small wavelength internal tides, since during vessel movement toward the wave, the wavelength, altered by the Doppler effect, becomes shorter. The hydraulic jump is more weakly pronounced than for measurements at the first stage. On the Kara side, the wave direction corresponds with that of vessel movement.

#### CALCULATIONS WITH THE NUMERICAL MODEL

Numerical modeling of the generation and propagation of internal waves in the strait was performed to study the internal wave dynamics and the influence of the mean flow on them. The driving force during modeling is the barotropic tidal currents flowing over underwater slopes, which create periodic vertical shifts of isopycnic surfaces and thereby generate an internal tide wave. In addition, numerical modeling makes it

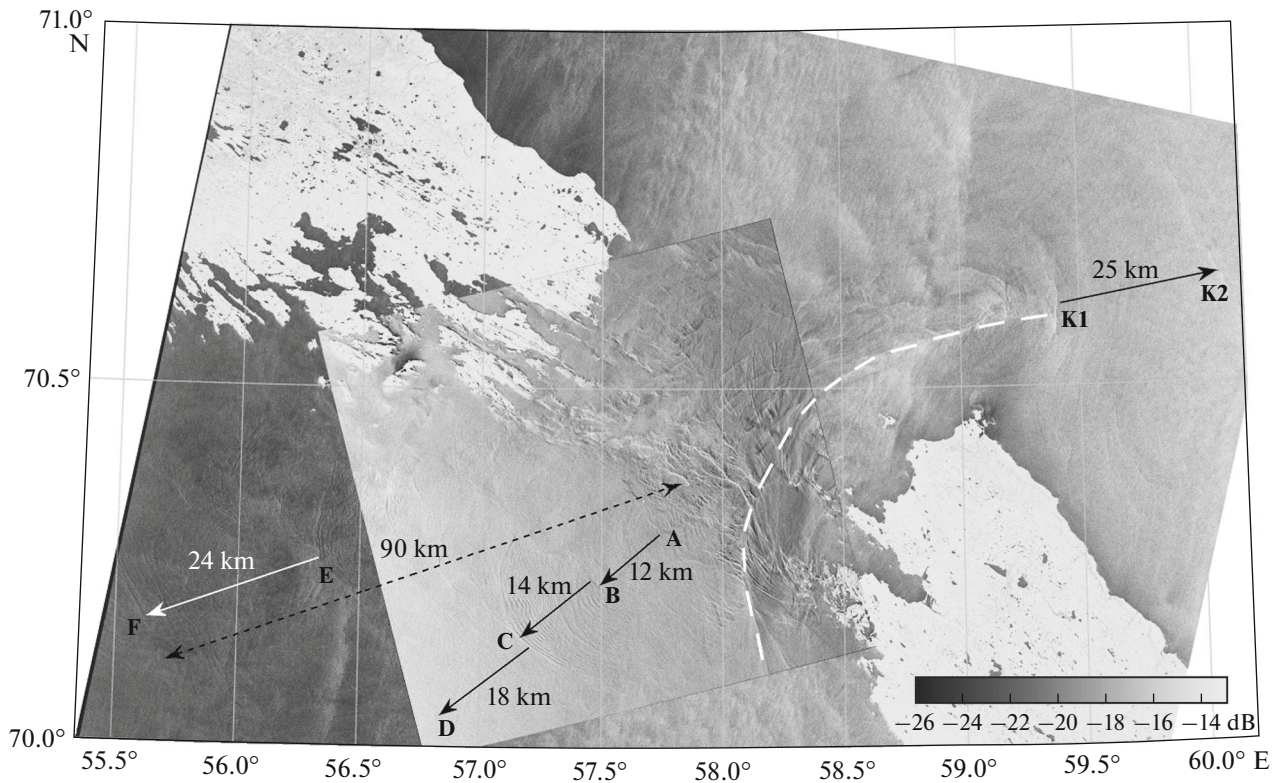


**Fig. 7.** Combined satellite radar images from Sentinel-1 SAR-C (0243 UTC) and ALOS-2 PALSAR-2 (1925 UTC) for October 1, 2015 in area of Kara Gates Strait. Letters A–F denote positions of short-period internal wave packets; K1, K2 denote surface manifestations of internal tide. White dotted line shows position of boundary of main current from Barents into Kara Sea. Images are given in terms of SEAD in dB. © ESA © JAXA.

possible to analyze internal wave propagation to both sides of the strait and study the properties and variability of a wave.

We used the numerical model developed by V. Vlasenko [1, 2, 8, 17, 20]. The equations of the model and the details of its use applied to internal waves in the Kara Gates are explained in [1, 15]. In this calculation, we used the bottom relief obtained from data from the towing legs. Density stratification was also taken from the towed CTD sounder measurement data. The current amplitude of the barotropic tide was taken equal to 9 cm/s, which corresponds to the estimate from satellite altimetry data [9]. The length of the calculation domain was 200 km, in order to a priori cover several wavelengths of internal semidiurnal waves. The horizontal step was 75 m and there were 20 vertical levels. The time step was 1.5 s. The horizontal viscosity and density diffusion coefficients were 12 m<sup>2</sup>/s above the ridge and 2 m<sup>2</sup>/s beyond it. The coefficients of vertical turbulent viscosity and density diffusion were 0.0001 m<sup>2</sup>/s. For smaller coefficients, instability in calculations occurs. A small step along the horizontal increases the nonlinearity, which suppresses dispersion at high latitudes.

We introduced into the model the mean flow from the Barents to the Kara Sea with a velocity of 12 cm/s

above the ridge, which occupied the entire water column, and periodic barotropic tidal currents with an amplitude of 9 cm/s were superposed on it. The barotropic tidal current velocities were estimated from satellite data. The ellipses of the tidal currents were taken from satellite data on the date the CTD transects [9]. The authors of [15] showed that these data coincide well with the buoy measurements [15]. Good coincidence is observed between them. Approximately the same ellipses with an amplitude of the major axis of around 9 cm were calculated in the numerical model [4] directly in the strait.

The perturbations of the density field in Fig. 8 are shown after calculations during three wave periods (36 h). Periodic barotropic tidal currents roll over the underwater slope, obtain the vertical components, and excite an internal wave. The pattern of the internal tide is asymmetric with respect to the ridge in the strait. From physical considerations it is clear that a stronger internal tide should be observed in the Barents Sea, since the wave from the ridge in the strait propagates opposite to the current. Precisely this is demonstrated by the numerical calculation. When the internal tide propagates opposite to the current, its amplitude increases owing to the decrease in the wavelength while retaining the energy of one wave period. East

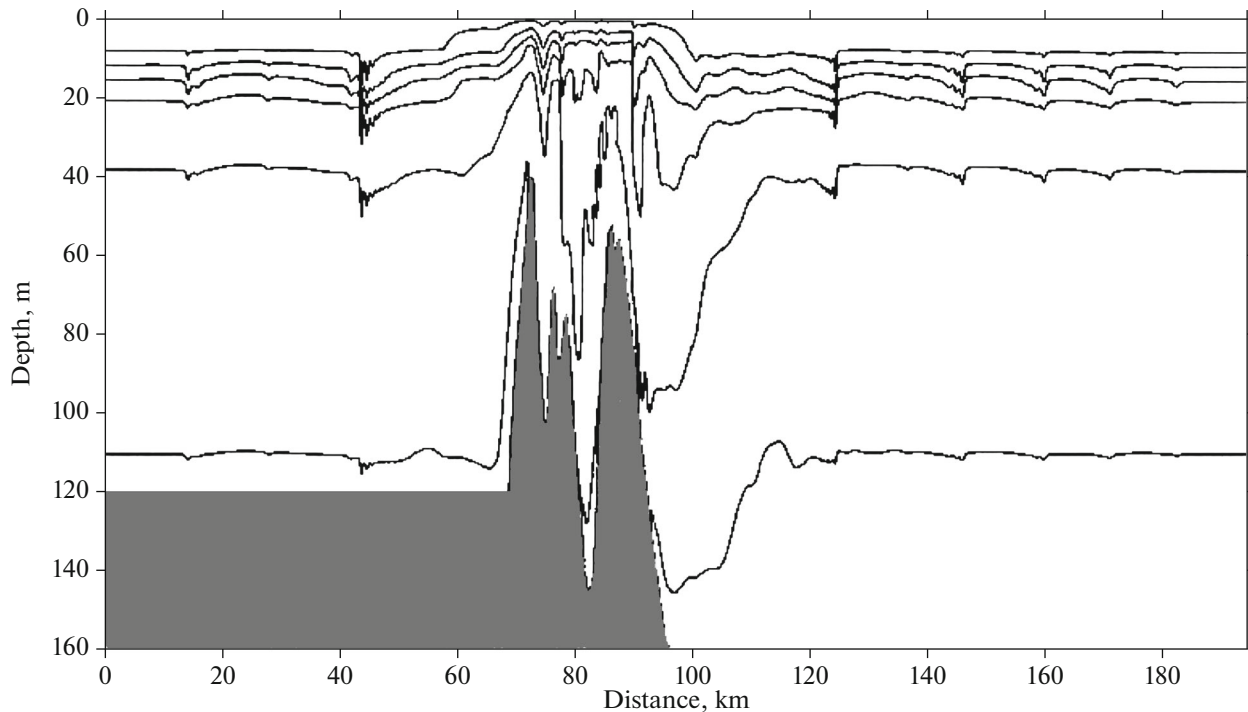


**Fig. 8.** Field of isopycnic surfaces 23, 24, 25, 26, and 27 units of arbitrary density disturbed by flow through strait and by passage of internal waves in accordance with numerical model calculations. Bottom relief in strait shown in gray.

and west of the threshold, an internal bore is observed (a sharp jump in the depth of isopycnic surfaces along the vertical). The isothermal and isopycnic surfaces dramatically deepen by 10–15 m. The internal bore manifests itself almost right near the ridge crest in the strait. Directly behind the internal bore, a packet of short-period waves occurs. To the left of the bore, the period of the internal tide wave is visible (the wavelength is around 17–18 km). Above it was shown that the wavelength, according to numerical calculations by the dispersion relation, is 23 km. Correction for the Doppler effect eliminates the differences between the model calculations and the dispersion relation.

From the Kara Sea side, the internal tidal wave from the strait propagates in the same direction as the current. This leads to a decrease in the wave amplitude and an increase in its wavelength. From the Kara side to the northeast of the ridge in the strait, a sudden deepening of the isopycnic surfaces is observed, which is a hydraulic jump that occurs in the flow behind an obstacle (Figs. 4, 5). Based on the numerical calculation data, isopycnic surface 27 deepens from 40 to 100 m. According to the measurement data, a similar pattern is observed (Fig. 4).

Density field fluctuations are not symmetrical on both sides of the strait (Fig. 5). Owing to the existence of the mean flow from the Barents Sea into the Kara, for opposite directions of the wave and the current in the Barents Sea, the wavelength decreases and the amplitude increases. The rising edge of the wave is gently sloping, and the trailing front is steep, which is

usually observed in internal waves [17]. At the trailing edge of an internal waves, an internal bore is formed. The isopycnals suddenly deepen, and behind them, a packet of short-period waves occurs. These high-frequency waves and internal bore cause spatially inhomogeneous vertical motions that manifest themselves on the surface in the form of areas without ripples where divergence of vertical flows is observed on the surface, and areas of ripples in convergence areas.

North of the strait, a hydraulic jump forms owing to the mean current flowing around the ridge into the Kara Sea. Numerical calculation of the wavelength of the internal tidal wave approximately corresponds to calculations by the dispersion relation and observations.

Behind the internal bore, a packet of short-period internal waves occurs. However, when the adopted technique of towed measurements in the scanning mode is used, short-period waves are not observed due to the cycle of lowering and raising of the device during towing, just like the wavelength of a short-period internal wave. The spatial resolution during towing is close to 900 m. The vessel moves at a speed of 6 kn, and the raising and lowering cycle of the sounder from the surface to the bottom is around 5 min. Within this time, the vessel covers a distance of around 900 m. The wavelength of short-period internal waves in the wave packet that occurs behind the internal bore are approximately equal to the distance that the vessel covers within each raising and lowering cycle of the device. Therefore the spatial resolution during such scanning is insufficient to describe such

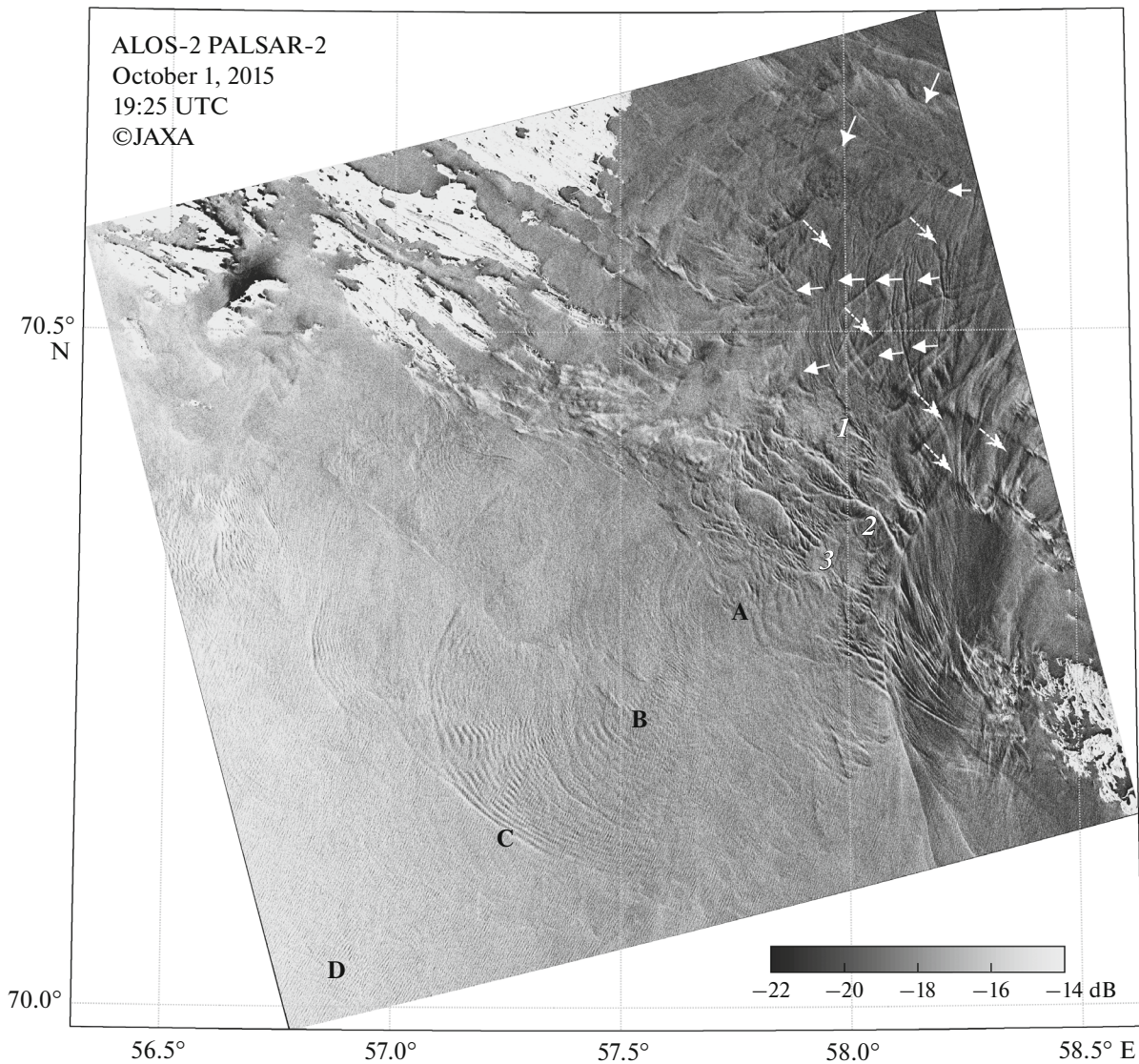


**Fig. 9.** Satellite radar image from ALOS-2 PALSAR-2 for October 1, 2015, showing detailed structure of field of internal waves in Kara Gates Strait and from Barents Sea side. Letters A–D and numerals 1–3 show positions of internal wave packets; arrows show direction of their propagation. Images are given in terms of SEAD in dB. © JAXA.

short-period waves. However, such waves are visible in radar imaging of the sea surface [14].

#### SATELLITE OBSERVATIONS

In the obtaining of additional information on the structure of the internal wave field in the Kara Gates Strait, we used satellite data with high spatial resolution (photos close in time to when the onboard measurements were conducted). For analysis, we used the radar imagery of a Sentinel-1 SAR-C with the spatial resolution of around 20 m (GG polarization, Interferometric Wide Swath imaging mode). Images were obtained on October 1, 2015 at 02:43 UTC for the Sentinel-1 and 19:25 UTC for the ALOS-2; the time difference between images was 16 h and 42 min.

Figures 7 and 9 show the fields of the specific effective area of dispersion (SEAD) of the radar image signal (in dB). The radar images of the Sentinel-1, which are larger in size ( $250 \times 150$  km), completely encompass the region of the Kara Gates Strait and the areas adjacent to it from the Barents and Kara sides. Imaging by the ALOS-2 image, ( $70 \times 70$  km in size), covers the central and southwestern parts of the strait from the Barents side. Combination of both radar images made it possible to obtain a more complete pattern of the tidal dynamics in the strait and on both sides of it. In the combined image, it is possible to clearly identify surface manifestations of short-period internal wave packets in the strait, their propagation to the southwest into the Barents Sea, and the propagation of internal tidal waves to the southeast into the Kara Sea. In addi-

tion, the radar images distinctly show the convergence zones of the current directed from the Barents into the Kara Sea. In Fig. 7, this is marked with a white dotted line and, according to satellite measurement data in the IF range, it corresponds to the southeastern periphery of the warm Barents Sea current.

The ALOS-2 image clearly shows surface manifestations of internal wave packets, which have a pronounced concentric shape and propagate from the strait to the west and southwest (Fig. 7). Analysis of the structure of internal wave manifestations in this radar image makes it possible to isolate four sequential short-period internal wave packets (denoted A, B, C, D), the distance between which increases with their propagation toward the Barents Sea. Packet A is at a distance of around 8 km from the assumed generation area above the threshold in the strait (marked by an \* in Fig. 7). Packets A-B, B-C, and C-D are at a distance of 12, 14, and 18 km from each other, which agrees well with the measured wavelengths of the internal tidal waves to the west of the strait. In the radar image, packet C is the most starkly pronounced, totaling around 30 solitons; the length of its front is around 40 km. Owing to the nonlinearity of short-period internal waves, the maximum wavelength in the packet corresponds to the leading wave and varies along its front within the limits of 400–800 m (see Fig. 9).

The Sentinel-1 radar image clearly shows another two internal wave packets E and F to the west of the strait; the distance between them is around 24 km. According to the satellite data, short-period internal wave packets propagate to a distance of 90–100 km from the assumed generation area in the strait (see Fig. 7). These observations confirm that the internal wave packets detected earlier in an Almaz-1 image in this area are caused not by local generation [3], but begin in the Kara Gates Strait [5]. Thus, the satellite images make it possible to trace five to six sequential tidal cycles of generation and propagation of high-frequency internal waves from the strait towards the Barents Sea.

From the Kara side to a distance of around 30 km to the west of the strait and farther, characteristic narrow curved bands of local intensification/attenuation of wind ripples are seen, directed to the northeast (denoted K1, K2 in Fig. 7). These manifestations do not have a pronounced packet structure like in the Barents Sea and are apparently a manifestation of the internal tide on the sea surface. The image distinctly shows two sequential signatures K1 and K2, the distance between which is around 24–26 km, which agrees well with the wavelength of the internal tide from the Kara side obtained during contact CTD measurements (Fig. 4). It is interesting to note that the direction of propagation of internal waves on both sides of the Strait are approximately located on the same axis, at an angle of 30°–40° clockwise with respect to the principal axis of the strait (see Fig. 7).

The ALOS-2 image also makes it possible to consider the detailed structure of internal waves in the strait (Fig. 9). At the entrance to the strait from the Kara Sea, several southwest-oriented solitons are observed. In the northwestern part of the strait from the Novaya Zemlya side, pronounced manifestations of short-period internal waves are hardly encountered at all. In the center of the strait, several groups of short-period waves in the opposite direction are observed, oriented across the strait (denoted by arrows in Fig. 9). The width of the packets directed from Vaygach Island toward Novaya Zemlya is 20–25 km; the width packets traveling in the opposite direction (toward Vaygach Island) are around 10 km. The distance between neighboring packets in both cases does not exceed 3–5 km. Generation of waves propagating across the strait is apparently explained by the interaction of the tidal current with the complex bottom topography and the presence of underwater ridges along and across the strait.

In the southwestern part of the strait, a series of short packets of internal waves directed into the Barents Sea is observed. Judging from all this, it is these packets that yield the onset of packets A–F considered above. It is quite complicated to isolate the three main packets (denoted 1, 2, 3 in Fig 9). Their wavelength is 1–2 km, and their width is 20–25 km; there are three to five waves in packets, and the distance between them is around 4–6 km. These packets occupy almost all of the central part of the strait up to the shallow-water areas close to Vaygach Island. Approximately 10 km from the southwestern end of Vaygach Island, the structure of internal waves shows a characteristic discontinuity owing to the shift in velocity at the boundary of the current directed from the Barents to the Kara Sea. East of the current boundary, surface manifestations of short-period internal waves are strongly diffuse.

Note that the leading waves in packets 1–3 have very large radar image contrasts. The distances between packets 1–3 approximately coincide with the distances between neighboring peaks of underwater ridges in this area of the strait (see profile 1–4 in Fig. 4). The generation of these packets obviously occurs as barotropic tidal currents flow over underwater slopes, as shown in the model calculation in Fig. 7. The high radar image contrasts of the observed waves are caused by the formation on intense areas of convergence of vertical flows, in which there occurs a sharp intensification of backscattering by short wind ripples and breakers [11, 12]. The particular sharpness of the convergence zones in this area is obviously explained by the high velocities of orbital currents on the surface with deepening of the tidal flow behind and obstacle and the oncoming motion of the Barents Sea current.

## CONCLUSIONS

Analysis of measurements using a towed CTD sounder and satellite images and the results of numer-

ical modeling show that in the area of the Kara Gates Strait, intense internal waves exist. Owing to the presence of a constant mean current from the Barents into the Kara Sea, the internal wave propagating into the Barents Sea is intensified. Due to the counter current, the wavelength decreases and the amplitude increases. In the area of the strait, nonlinear wave transformation occurs and short-period wave packets form, which are seen on the surface in satellite images. In the eastern part of the strait on the Kara side, a hydraulic jump is detected with deepening of the isotherms and isopycnals to 100 m. The bottom relief in the strait strongly differs from the digital data files of the bottom relief in different databases. The difference lies in the underwater ridge across the strait, which is a continuation of the Ural Mountains.

#### ACKNOWLEDGMENTS

This work (analysis of onboard measurement data and modeling) was supported by the Russian Science Foundation, grant no. 14-05-00095. Field works were supported by the Russian Foundation for Basic Research, project nos. 1 14-05-05003\_Kar\_a and 14-05-05006\_Kar\_a.

The authors thank the crew of the R/V *Akademik Mstislav Keldysh* for aid in conducting field works. Processing and analysis of satellite images was supported by the Russian Foundation for Basic Research, project no. 16-35-60072\_mol\_a\_dk, and partially by state order no. 5.2483.2014/K.

Identification and analysis of internal waves was supported by a grant from the President of the Russian Federation for government support of young scientists, MK-5562.2016.5.

ALOS-2 and PALSAR satellite data were obtained by the authors from the Japanese Aerospace Exploration Agency (JAXA) within the frameworks of projects PI no. 1193 and PI no. 3395 (fourth and sixth ALOS RA for ALOS-2). Sentinel-1 satellite data are the property of the European Space Agency and the European Commission and were obtained by the authors under free access conditions for scientific research.

#### REFERENCES

1. V. I. Vlasenko, "The nonlinear model of generation of baroclinic tides over extended heterogenic bottom relief," *Morsk. Gidrofiz. Zh.*, No. 6, 9–16 (1992).
2. V. I. Vlasenko and E. G. Morozov, "Generation of semidiurnal internal waves near a submarine ridge," *Okeanologiya (Moscow)* **33**, 282–286 (1993).
3. A. V. Dikinis, A. Yu. Ivanov, I. G. Mal'tseva, et al., "Encoding of internal waves on radar images of *Almaz-I* satellite using hydrometeorological and hydrographic data," *Issled. Zemli Kosmosa*, No. 5, 47–59 (1996).
4. B. A. Kagan and A. A. Timofeev, "Modeling of stationary circulation and semidiurnal surface and internal tides in the Kara Strait," *Fundam. Prikl. Girdofiz.* **8** (3), 72–79 (2015).
5. I. E. Kozlov, V. N. Kudryavtsev, E. V. Zubkova, A. V. Zimin, and B. Chapron, "Characteristics of short-period internal waves in the Kara Sea inferred from satellite SAR data," *Izv., Atmos. Ocean. Phys.* **51**, 1073–1087 (2015).
6. E. G. Morozov, "Internal tides in the Gibraltar and Bab-el-Mandeb straits," *Fundam. Prikl. Gidrofiz.* **8** (3), 26–30 (2015).
7. E. G. Morozov, V. G. Neiman, and A. D. Shcherbinin, "Internal tide in the Kara Strait," *Dokl. Earth Sci.* **393**, 1312–1314 (2003).
8. E. G. Morozov and S. V. Pisarev, "Internal tides at the Arctic latitudes (numerical experiments)," *Oceanology (Engl. Transl.)* **42**, 153–161 (2002).
9. G. D. Egbert and S.Y. Erofeeva, "Efficient inverse modeling of barotropic ocean tides," *J. Atmos. Oceanic Technol.* **19** (2), 183–204 (2002).
10. I. H. Harms and M. J. Karcher, "Modeling the seasonal variability of the hydrography and circulation in the Kara Sea," *J. Geophys. Res.: Oceans* **104** (6), 13431–13448 (1999).
11. V. Kudryavtsev, I. Kozlov, B. Chapron, and J. A. Johannessen, "Quad-polarization SAR features of ocean currents," *J. Geophys. Res.* **119** (9), 6046–6065 (2014). doi 10.1002/2014JC010173
12. V. Kudryavtsev, I. Kozlov, B. Chapron, and J. A. Johannessen, "Quad-polarized SAR measurements of ocean currents in C- and L-bands," *Proceedings of Geoscience and Remote Sensing Symposium* (Milan, 2015), pp. 4212–4215. doi 10.1109/IGARSS.2015.7326755
13. T. A. McClimans, D. R. Johnson, M. Krosshavn, et al., "Transport processes in the Kara Sea," *J. Geophys. Res.* **105**, 14121–14139 (2000).
14. E. G. Morozov, V. T. Paka, and V. V. Bakhanov, "Strong internal tides in the Kara Gates Strait," *Geophys. Res. Lett.* **35**, L16603 (2008).
15. E. G. Morozov, G. Parrilla-Barrera, M. G. Velarde, and A. D. Scherbinin, "The Straits of Gibraltar and Kara Gates: a comparison of internal tides," *Oceanol. Acta* **26** (3), 231–241 (2003).
16. E. G. Morozov, K. Trulsen, M. G. Velarde, and V. I. Vlasenko, "Internal tides in the Strait of Gibraltar," *J. Phys. Oceanogr.* **32**, 3193–3206 (2002).
17. E. G. Morozov, and V. I. Vlasenko, "Extreme tidal internal waves near the Mascarene Ridge," *J. Mar. Syst.* **9** (3–4), 203–210 (1996).
18. V. K. Pavlov and S. L. Pfirman, "Hydrographic structure and variability of the Kara Sea: implications for pollutant distribution," *Deep-Sea Res.* **42**, 1369–1390 (1995).
19. W. H. F. Smith and D. T. Sandwell, "Global sea floor topography from satellite altimetry and ship depth soundings," *Science* **277**, 1956–1962 (1997). [http://topex.ucsd.edu/cgi-bin/get\\_data.cgi](http://topex.ucsd.edu/cgi-bin/get_data.cgi).
20. V. Vlasenko and K. Hutter, "Numerical experiments on the breaking of solitary internal waves over a slope-shelf topography," *J. Phys. Oceanogr.* **32**, 1779–1793 (2002).

*Translated by A. Carpenter*